ELSEVIER

Journal of Photochemistry and Photobiology A: Chemistry 102 (1997) 139–150

Journal of PHOTOCHEMISTRY AND PHOTOBIOLOGY A:CHEMISTRY

Structure and photophysical properties of novel ruthenium(II) complexes containing 6-substituted bipyridines

Leif Hammarström [a], Jan Alsins [a], Anna Börje [b], Thomas Norrby [b], Lian Zhang [c], Björn Åkermark [b,*]

[a] *Department of Physical Chemistry, University of Uppsala, Box 532, S-751 21 Uppsala, Sweden*
[b] *Department of Chemistry, Organic Chemistry, Royal Institute of Technology, S-100 44 Stockholm, Sweden*
[c] *Astra Arcus, S-151 85 Södertälje, Sweden*

Received 9 November 1995; accepted 29 April 1996

Abstract

A series of novel tris(bpy)ruthenium(II)-type complexes (where bpy = 2,2′-bipyridine) $Ru(bpy)_2$(6-carboxylato-2,2′-bpy) hexafluorophosphate, $Ru(bpy)_2$((2,2′-bpy-6-yl)-acetic acid) dihexafluorophosphate, $Ru(bpy)_2$(6-methoxycarbonyl-2,2′-bpy) dihexafluorophosphate, and $Ru(bpy)_2$(6-methyl-2,2′-bpy) dihexafluorophosphate were synthesised, and characterised by NMR spectroscopy, cyclic voltammetry, absorption and emission spectroscopy. The dominating effect of the substituent on the emission properties was an increased radiationless deactivation via metal-centered states, leading to a very short lifetime at 298 K. The degree of modification of the photophysical properties compared to those of $Ru(bpy)_3^{2+}$ followed the degree of geometric distortion introduced by the substituted ligand as suggested by NMR spectroscopy. In $Ru(bpy)_2$(6-carboxylato-2,2′-bpy) hexafluorophosphate, an abnormal temperature dependence of the rate of radiative decay was observed. This may probably be explained by participation of metal-to-ligand charge transfer (MLCT) states originating from different, non-equivalent ligands.

Keywords: Bipyridine; Photophysical properties; Ruthenium(II) complex; Structure

1. Introduction

During recent decades, a number of artificial molecular systems for the conversion of light energy into chemical energy have been studied [1]. These are generally based on metal complexes which, on electronic excitation, give a metal-to-ligand charge transfer (MLCT) state in which one electron has been transferred from the central metal atom to one of the ligands. The electron may be captured by acceptor molecules and utilized in secondary reactions. Much interest has been focused on the stabilization of the charge-separated product. In the natural photosynthetic reaction centre, this is accomplished by a sophisticated arrangement for multistep electron transfer following the primary electron transfer step, leading to charge separation across the reaction centre embedded in the biological membrane [2]. In an attempt to develop an artificial system, some progress has been made by the construction of supramolecular assemblies exhibiting photoinduced multistep electron transfer [3–5].

Several artificial systems have employed Ru(II) polypyridine complexes as sensitizers, and there has been much interest in learning how to modify the properties of the sensitizer and the arrangement of the donor and acceptor units of the supramolecular assembly. While most modifications are time independent (i.e. tuning of the state energies, variation of the relative orientation and type of link between the functional components), only a few examples exist of time-dependent modifications, e.g. change in the conformation of the supermolecule during the reaction. Conformational changes which do not alter the general structure of the supermolecule, in response to intramolecular photoinduced electron transfer (PET), are common [6]. Examples include cases in which the distance between the separated charges is subsequently decreased [7] or increased [8].

In the present study, we investigated the possibility of photoinduced conformational changes in derivatives of $Ru(bpy)_3^{2+}$ (Fig. 1; bpy, 2,2′-bipyridine). Thus we prepared a series of novel $Ru(bpy)_3^{2+}$-type complexes in which a potentially metal-coordinating substituent was present in the 6-position of one of the bpy ligands in the heteroleptic complexes **1–3**.

* Corresponding author. Tel.: +46 790 60 00; fax: +46 8 791 23 33.

1010-6030/97/$17.00
PII S1010-6030(96)04395-X

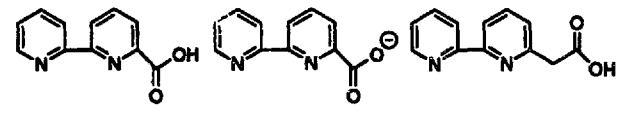

L1H, 6-carboxy-bpy L1, 6-carboxylato-bpy L2H, (bpy-6-yl)-acetic acid

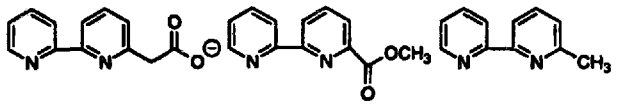

L2, (bpy-6-yl)-acetate L3, 6-methoxycarbonyl-bpy L4, 6-methyl-bpy

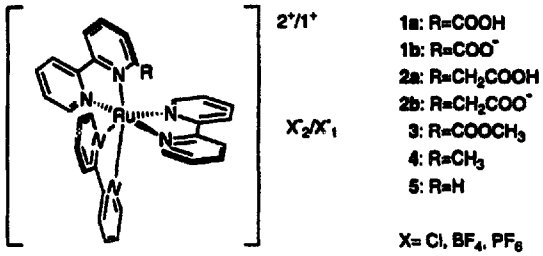

Fig. 1. Key to ligands and complexes.

The aim was to determine whether the substituent, e.g. carboxylate, which is free in the starting complex, could become coordinated after excitation and PET to an external or attached acceptor. The driving force for coordination is the increased attraction between the hard carboxylate donor (Pearson's HSAB notation) and the acceptor ruthenium, which becomes harder after oxidation to Ru(III). In addition, the preparation of a series of complexes with L1 (Fig. 1) shows that this is a very efficient terdentate ligand even for Ru(II) [9].

The coordination of carboxylate will lead to intramolecular ligand displacement of an adjacent bipyridine in the Ru(III) species formed after PET. If this displacement can be shown to occur, an electron acceptor may be covalently attached to the ligand to be displaced [10], and the ligand displacement will increase the distance between the reduced acceptor and Ru(III) (Scheme 1). Coordination of a carboxylate group will also decrease the positive charge on ruthenium, reducing the electron affinity of Ru(III). Both effects will potentially serve to decrease the rate of electron back transfer from the reduced acceptor to Ru(III) (the reduced electron affinity of Ru(III) results in a less exergonic back electron transfer from the reduced acceptor; provided that the acceptor is chosen so that the reaction is not in the Marcus inverted region, this may result in a smaller rate constant) [11]. It should be noted that photoinduced dissociation and substitution of ligands in Ru(II) polypyridine complexes are generally believed to proceed via short-lived, metal-centred states, with little or no possibility of intramolecular electron transfer. On the other hand, in the presently proposed reaction, the intramolecular ligand displacement reaction will occur subsequent to oxidative quenching of the excited state. Thus it may also occur in electrochemically oxidized complexes, and cyclic voltammetry was performed in order to investigate this possibility.

The introduction of ligands which distort the octahedral geometry of $Ru(bpy)_3^{2+}$ derivatives reduces the lifetime of the lowest excited ^{3}MLCT state due to the decreased activation energy for population of short-lived, metal-centred state(s) [12]. A general explanation for this observation is that, due to the distorted geometry, the ligand field is perturbed so that the activation energy for excited state deactivation via short-lived, metal-centred states becomes small. In the present study, the expected decrease in the excited state lifetime is not necessarily critical, since the system may be designed in such a way that the desired PET to the acceptor is rapid enough to compete with the other decay pathways of the excited state [3]. Furthermore, the complexes studied here all contain two unsubstituted bipyridines and one with a single substituent, whereas in earlier studies the substituents in the 6-position were either fairly large (e.g. phenyl) [13–15] or (for example, methyl) were present in both the 6- and 6′-positions and/or on all ligands of the complex [16].

The geometric distortion in the present complexes should be moderate. We examined the photophysical properties of **1–3** at temperatures between 298 and 100 K in order to establish the influence of the sterically demanding substituents. Specifically, we were interested in the excited state lifetime in this temperature interval, since it limits the time during which intramolecular PET may be competitive. Complex **4**, with a 6-methyl substituent, was included as reference with a relatively small distortion, and comparison was made with the parent complex $Ru(bpy)_3^{2+}$ (**5**). Thus, aided by information from two-dimensional (2D) nuclear magnetic resonance (NMR) spectroscopy, we were able to examine the relationship between the degree of geometric distortion and the degree of perturbation of the photophysical properties.

2. Experimental section

2.1. Materials

Ethanol (99.5%) was used as supplied by Kemetyl, Sweden. Diethyl ether, ethyl acetate and dichloromethane were

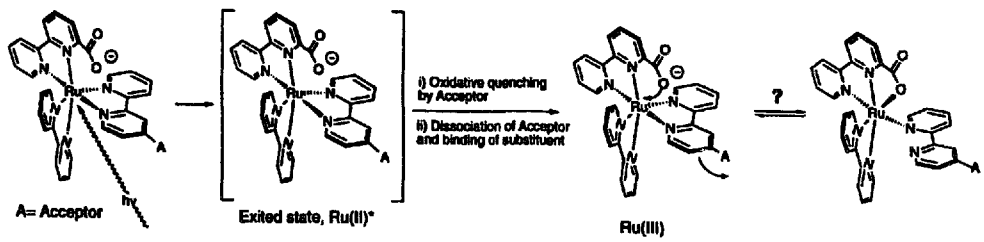

Scheme 1.

supplied by Kebo AB, Sweden, grade purum, and were distilled prior to use. Deionized water was used in all the experiments. All other solvents were of Aldrich high performance liquid chromatography (HPLC) grade unless stated otherwise. Column gel chromatography was performed on Aldrich alumina (neutral, 150 mesh, Brockmann activity type I). The ruthenium complexes **1–3** were prepared by reaction of the appropriate substituted bpy ligand [17] with bis-(bpy)ruthenium(II) dichloride dihydrate, prepared by a literature method [18] (characterized by NMR). Compound **4** was prepared from 6-methyl-bpy [19] and the ruthenium species above. The complexes **1–5** were characterized by NMR spectroscopy, UV–visible absorption spectroscopy, emission spectroscopy, redox potentials and elemental analysis. Nuclear Overhauser effect (NOE) spectroscopy was utilized to elucidate the connectivity between the pyridine rings in the bipyridines of complexes **1b, 2a, 3** and **4**. The assignment of the separate pyridine rings was possible using either COSY or DQF techniques. The annotation of the separate protons is identical to that presented (Fig. 5) in Section 4.

2.2. Synthesis

2.2.1. *Ru(2,2'-bipyridine)$_2$(6-carboxylato-2,2'-bipyridine) hexafluorophosphate (1b)*

A solution of bis(bpy)ruthenium(II) dichloride dihydrate (1.0 g, 1.92 mmol) and L1H (6-carboxy-bpy) (0.640 g, 3.20 mmol) in ethanol (99.5%, 35 ml) was degassed and then refluxed under argon for 5 h. After cooling, the solution was filtered to remove any unreacted $Ru(bpy)_2Cl_2$, and the solvent was evaporated at a rotary evaporator. The residue was dissolved in an aqueous solution of KPF_6, and a precipitate soon formed. It was subsequently filtered off and washed with cold water. This precipitate was dissolved in hot ethanol, and an orange–red solid **1b** was obtained by ether diffusion in a closed vessel. The product **1b** was filtered off, washed with a small amount of cold water and air dried (0.963 g, 1.27 mmol, 66%). This material was used for photophysical measurements after yielding satisfactory ^{1}H- and ^{13}C-NMR data. It was shown by voltammetry to exist as **1b** (deprotonated carboxylato ligand L1) in the electrochemical experiments. The complex **1a** was prepared for NMR and spectroscopic experiments by the addition of small amounts of trifluoroacetic acid (Aldrich, 99%) directly to the samples investigated.

UV–visible absorption spectra: **1a**, $\lambda_{max}=447$ nm, $\epsilon=11\,200\ M^{-1}\ cm^{-1}$ (in the presence of 40 mg trifluoroacetic acid in 3 ml spectroscopic solvent mixture); **1b**, $\lambda_{max}=453$ nm, $\epsilon=11\,400\ M^{-1}\ cm^{-1}$. In an effort to obtain X-ray quality crystals and material of satisfactory analytical purity, ion exchange in subsequent batches was performed utilizing concentrated aqueous solutions of $NaBF_4$, KPF_6 or NH_4PF_6. Recrystallization from water–ethanol or slow evaporation of water–ethanol, water–acetone or water–acetonitrile solutions failed to give single crystals of **1a** or **1b**. One sample of **1b**, obtained by treatment of an aqueous solution with KPF_6, yielded satisfactory ^{1}H-NMR and ^{13}C-NMR data.

^{1}H-NMR (400 MHz, methanol-d_4–acetone-d_6 (1 : 1 by volume)). Bpy-1: 8.78 (1H, dd, *J*: 1.3, 8.1, H3a), 8.20 (1H, dd, *J*: 7.8, 8.1, H6a), 7.68 (1H, dd, *J*: 1.3, 7.8, H5a), 8.78 (1H, ddd, *J*: 0.8, 1.3, 8.2, H3b), 8.46 (1H, ddd, *J*: 1.3, 5.6, 7.6, H5b), 8.15 (1H, ddd, *J*: 1.5, 7.6, 8.2, H4b), 7.74 (1H, ddd, *J*: 0.8, 1.5, 5.6, H6b). Bpy-2: 8.73 (1H, ddd, *J*: 0.8, 1.3, 8.1, H3c), 8.52 (1H, ddd, *J*: 0.8, 1.6, 5.6, H6c), 8.16 (1H, ddd, *J*: 1.6, 7.7, 8.1, H4c), 7.53 (1H, ddd, *J*: 1.3, 5.6, 7.7, H5c), 8.70 (1H, ddd, *J*: 0.8, 1.3, 8.2, H3x), 8.08 (1H, ddd, *J*: 1.5, 7.6, 8.2, H4x), 7.68 (1H, ddd, *J*: 0.8, 1.5, 5.7, H6x), 7.39 (1H, ddd, *J*: 1.3, 5.7, 7.6, H6x). Bpy-3: 8.63 (1H, ddd, *J*: 0.9, 1.3, 8.2, H3y), 8.09 (1H, ddd, *J*: 1.5, 7.6, 8.2, H4y), 7.66 (1H, ddd, *J*: 0.9, 1.5, 5.6, H6y), 7.42 (1H, ddd, *J*: 1.3, 5.6, 7.6, H5y), 8.52 (1H, ddd, *J*: 0.7, 1.3, 8.1, H3z), 8.00 (1H, ddd, *J*: 1.5, 7.6, 8.1, H4z), 7.65 (1H, ddd, *J*: 0.7, 1.5, 5.7, H6z), 7.34 (1H, ddd, *J*: 1.3, 5.7, 7.6, H5z).

^{13}C-NMR (d_6-acetone–d_4-methanol (1 : 1 by volume), 100 MHz carbon): 166.5, 158.5, 158.4, 155.7, 153.8, 152.7, 151.7, 140.1, 139.3, 139.1, 139.0, 138.8, 128.8, 128.7, 128.4, 128.1, 127.8, 126.9, 126.2, 125.6, 125.5, 125.2, 125.0, 124.2. One sample obtained by treatment with NH_4PF_6 gave the following elemental analysis: C, 43.15; H, 2.89; N, 9.71; this is indicative of chiefly protonated ligand L1H (**1a**, two PF_6 units) with some **1b** present. Calculated for **1a**: $C_{31}H_{24}N_6O_2RuP_2F_{12}$; C, 41.2; H, 2.68; N, 9.30. Calculated for **1b**: $C_{31}H_{23}N_6O_2RuPF_6$; C, 49.15; H, 3.06; N, 11.09.

2.2.2. *Ru(2,2'-bipyridine)$_2$((2,2'-bipyridine-6-yl)-acetic acid) dihexafluorophosphate (2a)*

A solution of bis(bpy)ruthenium(II) dichloride dihydrate (1.00 g, 1.92 mmol) and L2H ((bpy-6-yl)-acetic acid) (0.680 g, 3.17 mmol) in ethanol (99.5%, 35 ml) was degassed and then refluxed under argon for 5 h. After cooling, the solvent was evaporated at a rotary evaporator, leaving a fine red solid. A portion of the solid (approximately 60%) was dissolved in water and treated with a saturated aqueous solution of KPF_6, yielding a voluminous red precipitate on standing overnight. It was filtered off, redissolved in acetonitrile and precipitated by the addition of ethanol, followed by reduction of the volume and cooling. The red solid thus obtained was washed with cold water, redissolved in acetone and crystallized by ether diffusion in a closed vessel, yielding **2a** (0.643 g, 0.7 mmol, approximately 60% from the crude product). The mother liquid yielded successive crops of less pure material. The complex **2a** gave satisfactory ^{1}H-NMR and ^{13}C-NMR data and X-ray quality crystals [20] through ether diffusion (see above).

^{1}H-NMR (500 MHz, methanol-d_4–acetone-d_6 (1 : 1 by volume)). Bpy-1: 8.61 (1H, dd, *J*: 1.5, 8.0, H3a), 8.05 (1H, dd, *J*: 7.5, 8.0, H4a), 7.50 (1H, dd, *J*: 1.5, 7.5, H5a), 8.72 (1H, ddd, *J*: 0.8, 1.4, 8.4, H3b), 8.12 (1H, ddd, *J*: 1.5, 7.6, 8.4, H4b), 7.71 (1H, ddd, *J*: 0.8, 1.5, 5.7, H6b), 7.44 (1H, ddd, *J*: 1.4, 5.7, 7.6, H5b), 1.99 (2H, s, CH_2). Bpy-2: 8.76 (1H, ddd, *J*: 0.9, 1.3, 8.2, H3c), 8.19 (1H, ddd, *J*: 0.8, 1.5,

5.6, H6c), 8.15 (1H, ddd, *J*: 1.5, 7.6, 8.2, H4c), 7.55 (1H, ddd, *J*: 1.3, 5.6, 7.6, H5c), 8.72 (1H, ddd, *J*: 0.8, 1.4, 8.3, H3x), 8.12 (1H, ddd, *J*: 1.5, 7.6, 8.3, H4x), 7.73 (1H, ddd, *J*: 0.8, 1.5, 5.7, H6x), 7.43 (1H, ddd, *J*: 1.4, 5.7, 7.6, H5x). Bpy-3: 8.70 (1H, ddd, *J*: 0.8, 1.4, 8.2, H3y), 8.09 (1H, ddd, *J*: 1.5, 7.6, 8.2, H4y), 7.98 (1H, ddd, *J*: 0.8, 1.5, 5.7, H6y), 7.43 (1H, ddd, *J*: 1.4, 5.7, 7.6, H5y), 8.74 (1H, ddd, *J*: 0.8, 1.4, 8.2, H3z), 8.15 (1H, ddd, *J*: 1.5, 7.6, 8.2, H4z), 7.81 (1H, ddd, *J*: 0.8, 1.5, 5.6, H6z), 7.51 (1H, ddd, *J*: 1.4, 5.6, 7.6, H5z).

^{13}C-NMR (d_6-acetone, 100 MHz carbon): 166.2, 159.3, 158.4, 158.1, 157.8, 154.0, 152.7, 152.4, 152.3, 152.2, 139.3, 139.2, 138.9, 138.8, 138.6, 129.5, 129.0, 128.8, 128.6, 128.2, 125.7, 125.5, 125.4, 125.3, 122.9, 26.3. Elemental analysis: calculated for **2a**: $C_{32}H_{26}N_6O_2RuP_2F_{12}$; C, 41.89; H, 2.86; found: C, 42.33; H, 3.02. UV–visible absorption spectrum of **2a**: λ_{max}=449 nm, ϵ=15 000 M^{-1} cm^{-1}. It was shown by voltammetry to exist as **2a** (protonated carboxylate ligand L2H) in the electrochemical experiments. The complex **2b** was obtained in the emission studies by the addition of a small amount of aqueous NaOH to the spectroscopic sample.

2.2.3. *Ru(2,2'-bipyridine)$_2$(6-methoxycarbonyl-2,2'-bipyridine) dichloride·4H$_2$O and dihexafluorophosphate (3)*

A solution of bis(bpy)ruthenium(II) dichloride dihydrate (0.484 g, 0.96 mmol) and L3 (6-methoxycarbonyl-bpy) (0.321 g, 1.5 mmol) in methanol (99%, 20 ml) was degassed and then refluxed under argon for 6 h. After cooling, the solvent was evaporated at a rotary evaporator. The residue was recrystallized from acetone–dichloromethane to yield red crystals (0.141 g, 0.18 mmol, 19%). The mother liquid was evaporated and the residue yielded a second crop (0.166 g, 0.22 mmol, 23%) after chromatography on alumina (eluted with a gradient of 0–10 vol.% MeOH in CH_2Cl_2). Analysis: calculated for $C_{32}H_{26}N_6O_2RuCl_2\cdot 4H_2O$: C, 49.9; H, 4.35; N, 10.9; found: C, 49.9; H, 4.35; N, 10.1.

^{1}H-NMR (400 MHz, methanol-d_4). Bpy-1: 8.88 (1H, dd, *J*: 1.3, 8.5, H3a), 8.25 (1H, dd, *J*: 7.7, 8.5, H4a), 7.73 (1H, dd, *J*: 1.3, 7.7, H5a), 8.84 (1H, ddd, *J*: 0.8, 1.3, 8.2, H3b), 8.19 (1H, ddd, *J*: 1.5, 7.6, 8.2, H4b), 7.86 (1H, ddd, *J*: 0.8, 1.5, 5.7, H6b), 7.49 (1H, ddd, *J*: 1.3, 5.7, 7.6, H5b), 3.20 (3H, s, OMe). Bpy-2: 8.78 (1H, ddd, *J*: 0.8, 1.3, 8.2, H3c), 8.46 (1H, ddd, *J*: 0.8, 1.5, 5.7, H6c), 8.20 (1H, ddd, *J*: 1.5, 7.6, 8.2, H4c), 7.57 (1H, ddd, *J*: 1.3, 5.7, 7.6, H5c), 8.74 (1H, ddd, *J*: 0.8, 1.3, 8.2, H3x), 8.12 (1H, ddd, *J*: 1.5, 7.6, 8.2, H4x), 7.62 (1H, ddd, *J*: 0.8, 1.5, 5.7, H6x), 7.40 (1H, ddd, *J*: 1.3, 5.7, 7.6, H5x). Bpy-3: 8.62 (1H, ddd, *J*: 0.7, 1.4, 8.2, H3y), 8.05 (1H, ddd, *J*: 1.5, 7.6, 8.2, H4y), 7.67 (1H, ddd, *J*: 0.7, 1.5, 5.7, H6y), 7.41 (1H, ddd, *J*: 1.4, 5.7, 7.6, H5y), 8.70 (1H, ddd, *J*: 0.8, 1.3, 8.2, H3z), 8.13 (1H, ddd, *J*: 1.5, 7.6, 8.2, H4z), 7.64 (1H, ddd, *J*: 0.8, 1.5, 5.7, H6z), 7.46 (1H, ddd, *J*: 1.3, 5.7, 7.6, H5z).

^{13}C-NMR (d_4-methanol, 100 MHz carbon): 165.2, 160.0, 159.0, 158.7, 158.3, 157.0, 154.0, 152.8, 152.6, 152.0, 140.5, 139.7, 139.5, 139.4, 139.1, 129.1, 129.0, 128.7, 128.4, 127.8, 53.6. UV–visible absorption spectrum of **3**: λ_{max}=445 nm, ϵ=10 800 M^{-1} cm^{-1}. To a portion of the product dissolved in water, an excess (2–3 ml) of a saturated aqueous solution of KPF_6 was added. The orange–red precipitate formed was filtered off, washed with water and acetone and dried in vacuo at the pump. It yielded satisfactory ^{1}H-NMR data, and was used in the emission studies.

2.2.4. *Ru(2,2'-bipyridine)$_2$(6-methyl-2,2'-bipyridine) dihexafluorophosphate (4)*

A solution of bis(bpy)ruthenium(II) dichloride dihydrate (0.508 g, 1.0 mmol) and L4 (6-methyl-bpy) (0.239 g, 1.4 mmol) [19] was degassed and then refluxed in ethanol (99.5%, 25 ml) under argon for 4 h. After cooling, the solvent was evaporated at a rotary evaporator and the solid residue was extracted with ether to remove unreacted ligand. The solid residue was dissolved in hot water and an excess (2–3 ml) of a saturated aqueous solution of KPF_6 was added. The precipitate formed on cooling was filtered off and recrystallized from ethyl acetate–acetone to yield product **4** (0.667 g, 0.76 mmol, 75%). Analysis: calculated for $C_{31}H_{26}N_6RuP_2F_{12}$: C, 42.62; H, 3.00; N, 9.62; found: C, 42.54; H, 3.02; N, 9.50.

^{1}H-NMR (500 MHz, methanol-d_4–acetone-d_6 (1 : 1 by volume)). Bpy-1: 8.60 (1H, dd, *J*: 1.4, 8.2, H3a), 8.05 (1H, dd, *J*: 7.8, 8.2, H4a), 7.49 (1H, dd, *J*: 1.4, 7.8, H5a), 8.72 (1H, ddd, *J*: 0.8, 1.4, 8.3, H3b), 8.11 (1H, ddd, *J*: 1.5, 7.6, 8.3, H4b), 7.73 (1H, ddd, *J*: 0.8, 1.5, 5.7, H6b), 7.42 (1H, ddd, *J*: 1.4, 5.7, 7.6, H5b), 1.99 (3H, s, Me). Bpy-2: 8.76 (1H, ddd, *J*: 0.8, 1.3, 8.2, H3c), 8.19 (1H, ddd, *J*: 0.8, 1.5, 5.5, H6c), 8.17 (1H, ddd, *J*: 1.5, 7.6, 8.2, H4c), 7.54 (1H, ddd, *J*; 1.3, 5.5, 7.6, H5c), 8.71 (1H, ddd, *J*: 0.8, 1.4, 8.3, H3x), 8.12 (1H, ddd, *J*: 1.5, 7.6, 8.3, H4x), 7.71 (1H, ddd, *J*: 0.8, 1.5, 5.6, H6x), 7.44 (1H, ddd, *J*: 1.4, 5.6, 7.6, H5x). Bpy-3: 8.69 (1H, ddd, *J*: 0.8, 1.3, 8.3, H3y), 8.06 (1H, ddd, *J*: 1.5, 7.6, 8.3, H4y), 7.98 (1H, ddd, *J*: 0.8, 1.5, 5.7, H6y), 7.43 (1H, ddd, *J*: 1.3, 5.7, 7.6, H5y), 8.74 (1H, ddd, *J*: 0.8, 1.4, 8.3, H3z), 8.14 (1H, ddd, *J*: 1.5, 7.6, 8.3, H4z), 7.81 (1H, ddd, *J*: 0.8, 1.5, 5.6, H6z), 7.51 (1H, ddd, *J*: 1.4, 5.6, 7.6, H5z).

^{13}C-NMR (d_6-acetone, 100 MHz carbon): 159.5, 158.6, 158.5, 154.2, 152.8, 152.5, 152.4, 152.3, 139.3, 139.1, 138.9, 129.6, 128.9, 128.7, 128.3, 125.8, 125.7, 125.6, 125.5, 125.4, 123.1, 26.4. UV–visible absorption spectrum of **4**: λ_{max}-449 nm, ϵ=15 500 M^{-1} cm^{-1}.

2.2.5. *Ru(2,2'-bipyridine)$_3$ dichloride·2.5H$_2$O and dihexafluorophosphate (5)*

Product **5** was obtained as a byproduct in the synthesis of bis(bpy)ruthenium(II) dichloride dihydrate by the literature procedure [18], and gave satisfactory ^{1}H-NMR and UV–visible absorption spectra [21]: λ_{max}=450 nm, ϵ=13 700 M^{-1} cm^{-1}. To a portion of the product dissolved in water, an excess (2–3 ml) of a saturated aqueous solution of KPF_6 was added. The yellow–green precipitate formed was filtered off, washed with water and acetone and dried in vacuo at the

pump. It yielded satisfactory ^{1}H-NMR data, and was used in the emission studies.

2.3. Analyses

The analyses (carbon, hydrogen and nitrogen) were performed by Analytische Laboratorien GmbH, D-51789 Lindlar, Germany.

2.4. Methods

The NMR spectra of the complexes **1–5** were recorded in deuterated water, methanol, chloroform or acetone on Bruker AM 400 (400 MHz proton) or DMX 500 (500 MHz proton, 100 MHz carbon) instruments. Comprehensive studies of 2D experiments (observation of the NOE and DQF/COSY techniques (H–H correlation)) are being pursued and will be reported elsewhere [22].

2.5. Photophysical measurements

The absorption spectra were recorded in ethanol–methanol (4 : 1 by volume), ethanol (99.5% spectroscopic grade) and methanol (99.5% HPLC grade) using a Varian CARY 5E UV-VIS-NIR spectrophotometer.

For the temperature-dependent emission properties, the samples were placed in quartz ampoules (diameter, 5 mm) which were purged with N_2 and sealed. The solvent, ethanol–methanol (4 : 1 by volume), vitrifies to a glass in the 130–110 K region. The ampoules were placed in a nitrogen-cooled Oxford Instruments ND 1704 cryostat with a temperature control unit.

The emission spectra and quantum yields were determined using a SPEX Fluorolog 2 spectrofluorometer using an excitation wavelength of 452 nm and right angle detection. Correction factors for the wavelength-dependent sensitivity of the detection system were obtained using a lamp (General Electric DXW, 1000 W) calibrated by the Swedish National Testing and Research Institute [23].

For each complex, the temperature dependence of the quantum yield was determined in one series of measurements on the same sample, without changing the sample position. The values thus obtained were calibrated at 100 K against $Ru(bpy)_3^{2+}$, using samples with an absorbance of 0.100 at 452 nm (determined at 298 K) in a 1 cm rectangular cuvette. The cuvette could be accurately repositioned after removal from the cryostat, ensuring correct calibration. A value [12] of $\phi_{em}=0.38$ at 77 K was used for $Ru(bpy)_3^{2+}$. It was assumed that the differences in optical density and index of refraction above the glass transition temperature cancelled within experimental error [24]. It was also assumed that the solvent contracted to 80% of its volume on vitrification, resulting in an increased concentration. Because the absorbance was low, the quantum yield was approximately linearly dependent on the absorbance. Thus the values above the vitrification temperature were divided by 0.8. It must be emphasized that the uncertainty in the absolute quantum yields was generally assumed to be at least 20% [25]. In addition, the relative quantum yields should be considered with caution when changes in the solvent occur, such as in the present case.

Emission lifetimes were determined using an N_2 laser (LSI Laser Science, Inc., model VSL 337ND; $\lambda=337$ nm; pulse width, approximately 10 ns) or an excimer laser (Lambda Physik EMG 100; with XeCl; $\lambda=308$ nm; pulse width, approximately 15 ns). A Tektronix 7912 AD digitizer was used in the detector system. The shorter lifetimes were determined by single photon counting using the frequency-doubled emission ($\lambda=320$ nm) from a DCM dye laser synchronously pumped by a mode-locked Nd-YAG laser (Spectra Physics model 3800, $\lambda=530$ nm). The lifetimes of **1a** and **1b** were determined using both systems, and the values thus obtained agreed within experimental error.

All samples contained a second species with a high emission quantum yield. Although this was the minor component, it contributed significantly to the emission at room temperature for at least **1a**, **1b** and **3**. From the temperature dependence of the emission lifetime and wavelength maximum, this species was recognized as $Ru(bpy)_3^{2+}$, and the evaluation of the data obtained could readily be corrected for this contribution. The apparent quantum yield at 298 K showed that the $Ru(bpy)_3^{2+}$ content was no more than 2 mol.%. The time-resolved emission data were fitted to one or two single exponential functions using a SIMPLEX routine. Two exponentials were used only when the contribution from $Ru(bpy)_3^{2+}$ was significant, and the rate constant of the second exponential function was then fixed at the value for $Ru(bpy)_3^{2+}$ at that temperature. No sign of decomposition of the complexes was seen during the photophysical measurements.

2.6. Electrochemical measurements

Reduction potentials were determined using cyclic voltammetry in acetonitrile (anhydrous, less than 0.005% water, in Aldrich Sure/Seal™ bottles) with 0.1 M Bu_4NBF_4. The acetonitrile was syringe transferred to a nitrogen-flushed cell containing the electrolyte salt and the complex. A three-electrode system with glassy carbon (working) platinum wire (counter) and saturated calomel (SCE, reference) electrodes was used. The porous glass plug of the SCE was rinsed with water between each experiment to avoid the precipitation of salt due to acetonitrile entering the plug. It is important to note that a significant junction potential exists between acetonitrile and water in the SCE. As a consequence, the reduction potentials reported for $Ru(bpy)_3^{2+}$ vs. SCE in acetonitrile [26] and vs. a normal hydrogen electrode (NHE) in water [27] are very similar. The junction potential can be kept constant, which was carefully checked, and allows meaningful comparison between different complexes. Our values for the peak potentials of $Ru(bpy)_3^{2+}$ are in excellent agreement with previous reports [26].

Table 1
Photophysical data for the complexes

Compound	Absorption data [a]		Emission data [a]				
	λ (ϵ) (nm (cm^{-1} M^{-1}))		$\Phi_{298\ K}$	$\Phi_{100\ K}$ [b]	λ_{max} [c] (100 K) (nm)	ΔE_{max} [d] (100–140 K) (cm^{-1})	k_r [e] (s^{-1})
1a	447 (12000)	289 (65000)	$<1\times10^{-4}$	0.37	603	1500	1.0×10^{5}
1b	453 (11000)	290 (58000)	$<1\times10^{-4}$	0.28	595	1200	0.8×10^{5}
2	449 (15000)	289 (85000)	1×10^{-3}	0.43	582	1040	1.0×10^{5}
3	445 (10800)	288 (60000)	$<1\times10^{-4}$	0.31	612	1600	0.9×10^{5}
4	449 (15500)	289 (89000)	1×10^{-3}	0.43	582	1050	1.0×10^{5}
$Ru(bpy)_3^{2+}$	450 (14300) [f]	288 (81000)	0.07	0.45	580	1040	1.1×10^{5}

[a] In N_2-purged ethanol–methanol at 25 °C.
[b] Emission quantum yield.
[c] Wavelength of maximum emission intensity (corrected).
[d] Energy difference between the emission maxima at 100 and 140 K (below and above the glass transition temperature).
[e] Rate constant for radiative decay determined at 100 K according to Eq. (1).
[f] From Ref. [21].

3. Results

3.1. Absorption spectra

The absorption spectra of compounds **1–4** are very similar to that of $Ru(bpy)_3^{2+}$ (λ_{max} around 450 nm), but the weak band around 530 nm, originating from the direct transition to the ^{3}MLCT state, is observed only in the latter compound. The maximum wavelength and extinction coefficient for the dominant visible peak (transition to ^{1}MLCT) and the lowest band originating from ligand-centred transitions (π–π^*) are given in Table 1.

3.2. Emission properties

The emission lifetime and quantum yield were measured for all the compounds in N_2-purged ethanol–methanol (4 : 1 by volume) at several temperatures down to 77 K. At room temperature, the emission was weak and very short lived for the complexes **1–4** (Table 1), but as the temperature was decreased, both the emission lifetime (τ) and quantum yield (Φ) increased, especially when the solvent vitrified around 120 K.

The rate constant of emission decay as a function of temperature is shown in Fig. 2. In low-temperature glass, all complexes exhibited a similar relatively long lifetime (3–5 μs) which decreased slowly on heating. After a discontinuity at the glass transition, the weak temperature dependence continued. Around a certain temperature, different for the different complexes, the lifetime started to decrease dramatically with increasing temperature (Fig. 2).

Above 140 K, the emission quantum yield and lifetime showed a similar temperature dependence for all compounds except **1b**. This is expected when the rate constant for radiative deactivation k_r is temperature independent since

$$\Phi = k_r\tau \quad (1)$$

Eq. (1) is valid if the emitting state is formed with unit efficiency after excitation, as is usually assumed [28]. For **1b**, Φ exhibited a weaker dependence on the temperature than τ, as shown in Fig. 3. This means that k_r increased with increasing temperature even above 140 K, which is unusual

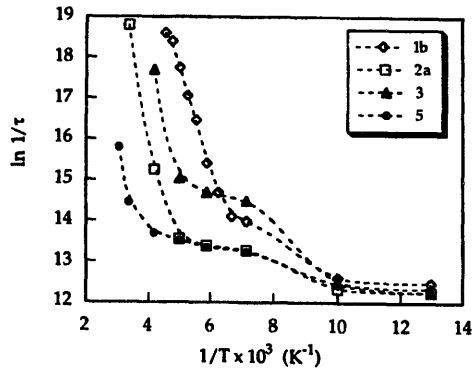

Fig. 2. Temperature dependence of the emission lifetime. The lines are guides to the eye. The lifetimes of **4** and **2b** follow that of **2a**. The temperature dependence of the lifetime of **1a** is shown in Fig. 3. The solvent (ethanol–methanol (4 : 1 by volume)) vitrifies at a temperature around 120 K, causing a discontinuous variation in the lifetime.

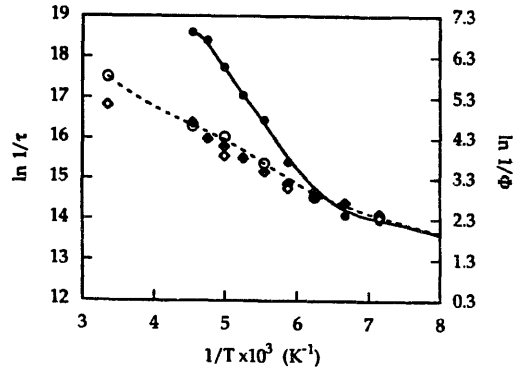

Fig. 3. Temperature dependence of the emission lifetime (filled symbols) and quantum yield (open symbols) for **1a** (diamonds) and **1b** (circles). The vertical axes are displaced by the value of ln k_r, according to Eq. (1). The lines are guides to the eye. The data show that k_r for **1b** is temperature dependent even above 140 K.

for $Ru(bpy)_3^{2+}$-type complexes [12]. The emission quantum yield was higher at 100 K than at 77 K for all complexes (**1a** and **3** not measured) and passed through a maximum between these temperatures. The values of k_r calculated according to Eq. (1) are given in Table 1.

The emission spectra of **1–4** at 100 and 140 K are shown in Fig. 4. On vitrification of the matrix, the emission maxima were blue shifted and the vibrational structure became more prominent. The energies of the emission maxima decreased in the order $Ru(bpy)_3^{2+} > 2 \approx 4 > 1b > 1a > 3$ at 100 K (**3** > **1a** at 140 K). The degree of vibrational structure was much lower for **1a** and **3** than for $Ru(bpy)_3^{2+}$. Furthermore, at the blue edge of the spectrum, the intensity increased more slowly with increasing wavelength, and the second vibrational peak increased relative to the first. This could also be seen to some extent for **1b**. The vibrational progression with a spacing of approximately 1300 cm^{-1} was the same for complexes **1b**, **2**, **4** and $Ru(bpy)_3^{2+}$. For **1a** and **3**, the spectra indicated a closer spacing, but the low degree of structure made this observation uncertain.

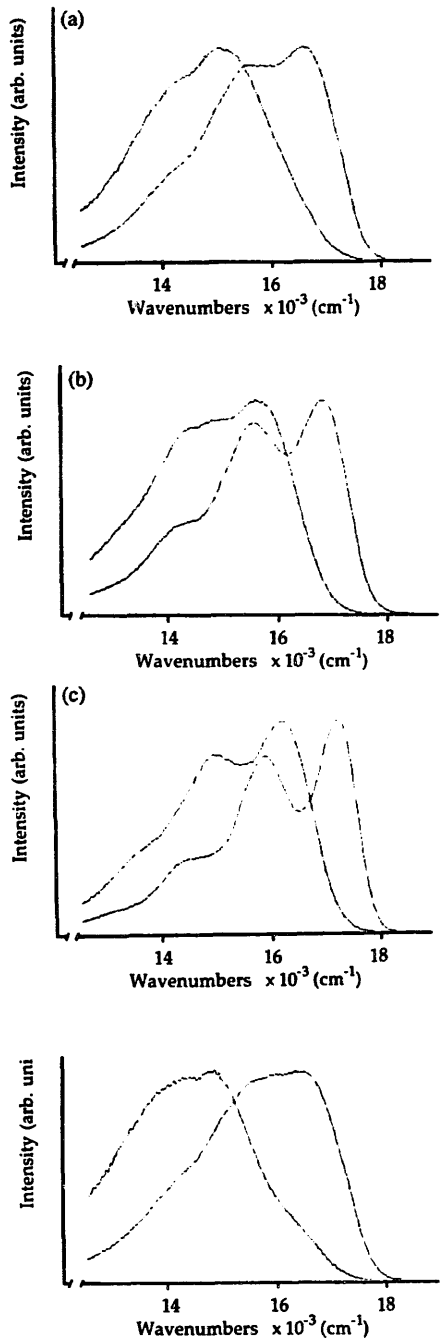

Fig. 4. Emission spectra at 100 K (higher energy) and 140 K (lower energy) for: (a) **1a**; (b) **1b**; (c) **2a**; (d) **3**. The spectra are arbitrarily scaled to show the shape and wavenumber shift. For comparison of the (integrated) intensity between the complexes, the emission quantum yield at 100 K is given in Table 1. The spectra of **2b** and **4** are identical to that of **2a**. The shapes of the spectra for **2** and **4** are identical to that of $Ru(bpy)_3^{2+}$, but are slightly red shifted (see Table 1).

Table 2
Reduction potentials (vs. SCE) for the complexes. Conditions: 0.1 M Bu_4NBF_4 in CH_3CN. **1a** and **2b**, which were obtained by the addition of acid or base, could not be measured

Complex	$E_{1/2}$(oxid.)	$E_{1/2}$(red.)		
		(1)	(2)	(3)
$Ru(bpy)_3^{2+}$	+1.31	−1.30	−1.49	−1.73
1b	+1.34	−1.40	−1.56	−1.94
2a	+1.34	−1.28	−1.49	−1.74
3	+1.38	−1.19	−1.46	−1.74
4	+1.31	−1.30	−1.50	−1.76

3.3. Electrochemical data

The reduction potentials vs. SCE for the different complexes in acetonitrile are shown in Table 2. The results for $Ru(bpy)_3^{2+}$ are in good agreement with previously reported values [26]. All complexes exhibited at least three reductions, corresponding to the successive reduction of each of the ligands, and one oxidation, corresponding to oxidation of the metal. The split in potential between the anodic and cathodic peaks for these redox steps never exceeded 80 mV (scan rate, 100–150 mV s^{-1}), indicating near-reversibility.

4. Discussion

4.1. Structure of the complexes

The assignment of the structure of complexes **1–4** was made principally from the NMR data, supported by visible spectroscopy. The absorption spectra are quite similar for all the compounds (**1–4** and also $Ru(bpy)_3^{2+}$). There is a strong absorption at about 450 nm and another at approximately 290 nm. In contrast, complexes in which one carboxylate is coordinated in the ground state give a ^{1}MLCT absorption of about 480 nm [9]. Because of the dissymmetry which is introduced by the 6-substituent in one of the bpy ligands, the connectivity between the different pyridine rings can be determined using NOE spectroscopy. Thus all signals in the proton NMR spectrum were assigned. The results show that the arrangement

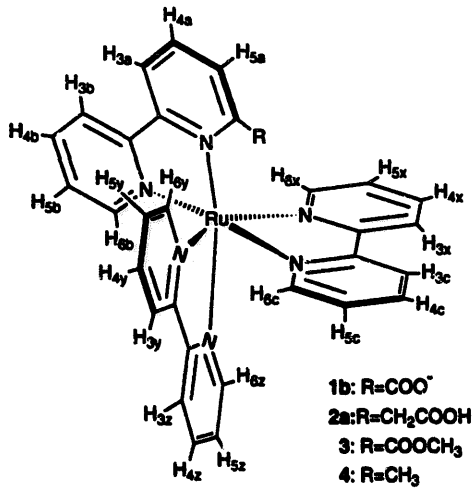

Fig. 5. Classification formalism for the protons of a substituted complex as referred to in the NMR discussions.

of the bipyridine units is similar in complexes **1–5**, supporting the conclusion that the substituent is not coordinated in the ground state of **1a** and **1b**. Furthermore, from the general appearance of the NOE (i.e. strength and number of protons experiencing NOE from their neighbouring protons), it appears that **1** and **3** are most severely distorted from D_3 symmetry (stronger interaction between H6b, H6x and H6z) (Fig. 5). Complexes **2** and **4** appear less geometrically distorted, because they show a smaller NOE between the H6b, H6x and H6z protons. Another observation in **2** and **4** is the NOE between H6c and H6y, the protons which are closest to the 6-substituent, an effect which is conspicuously absent in **1** and **3**. It is possible that it is due to a steric effect of the substituent in **1** and **3**, moving H6c and H6y too far away from each other for the NOE to be observed. Striking pairwise similarities are found in the entire sets of proton NMR data for, on the one hand, **1b** and **3** and, on the other, **2a** and **4**. This strongly supports the conclusion that substantial structural similarities exist within each of these two pairs. Unusually, downfield shifts (approximately 0.5 ppm) of H6c are observed in **1** and **3**, most probably due to the location of the carbonyl group. This is also observed in another ruthenium compound studied, where a large downfield shift (approximately 1 ppm) of a bpy 6-proton orthogonal to a coordinated carboxylate group is found [9].

4.2. Model for the emitting state of $Ru(bpy)_3^{2+}$

Before discussing the present results, it is necessary to describe the basic features of the currently established model [12,29,30] used to explain the photophysical and electrochemical properties of $Ru(bpy)_3^{2+}$ and its derivatives.

It is generally agreed that the emitting state of $Ru(bpy)_3^{2+}$ consists of a manifold of MLCT states. Three are low-lying, closely spaced ($\Delta E \approx 60$ cm^{-1}) states of mainly triplet character and different symmetries. These are responsible for the observed luminescence, and are populated within less than 10 ps with unit efficiency, independent of the excitation wavelength. Since the rate constants for both radiative and radiationless deactivation to the ground state are larger for the higher states, the Boltzmann distribution between the states gives rise to a complicated dependence on temperature for the excited state lifetime and emission quantum yield, especially below 100 K. This temperature dependence is believed to be the major reason for the decrease in lifetime on heating to approximately 200 K, except for the discontinuous change observed in the glass transition region of the solvent. At higher temperature, the drastic decrease in lifetime and emission quantum yield is explained by the population of a non-emissive, metal-centred (MC) triplet state with a very short lifetime. It is also believed that photosubstitution occurs via this state, with important implications for the use of $Ru(bpy)_3^{2+}$-type complexes as photosensitizers [31].

For $Ru(bpy)_3^{2+}$ itself, the temperature dependence of the rate of excited state decay above 84 K is described [12] by

$$k = k_r + k_{nr}^0 + k'_{nr} + \sum k_i \exp(-\Delta E_i/RT) \quad (2)$$

where k is the observed rate constant, k_r and k_{nr}^0 are the rate constants of radiative and radiationless decay determined at 84 K and k'_{nr} is an empirically found, temperature-dependent function describing the change in k_{nr} in the glass transition region of the solvent. Two Arrhenius terms are included to account for the population redistribution within the ^{3}MLCT manifold above 84 K and the deactivation through population of the ^{3}MC state respectively. The parameters for the latter process are $k_2 = 10^{13}$–10^{14} s^{-1} and $\Delta E_2 = 3600$–4000 cm^{-1}. Due to the short lifetime of the ^{3}MC state, this process contributes to a large extent to the excited state deactivation at room temperature, even though its fraction of the population is very small. Eq. (2), with similar interpretation and varying numbers of Arrhenius terms, has been used for other Ru(II) complexes with substituted bpy or similar ligands, but examples exist where Eq. (2) cannot be used at all [32].

Following some controversy, it is now established that, in fluid solution, the emitting ^{3}MLCT states are localized on one ligand [12,29,30,33], even if the rate of interligand electron transfer is high [34]. The situation is clear in crystals and rigid media, however [30,35,36]. One important consequence of localization is that, in complexes with different ligands, the ligand providing the lowest ^{3}MLCT states forms an emitting unit with the metal, whereas the other ligands act as spectators. Thus in many aspects this Ru–ligand couple behaves as an independent chromophore, with the spectator ligands only tuning the properties of the complex.

4.3. Assigning the emitting state

From the similar photophysical behaviour and spectral properties of complexes **1–4** and $Ru(bpy)_3^{2+}$, we assign the emitting state to ^{3}MLCT in all cases. For heteroleptic ruthenium polypyridine complexes, the ^{3}MLCT state is assumed to be localized on the most easily reduced ligand, as determined electrochemically. The reduction potentials of the dif-

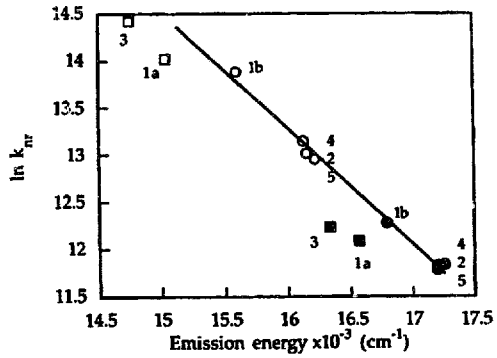

Fig. 6. Energy gap law. The values of ln k_{nr} were derived at 100 K (filled symbols) and 140 K (open symbols) from $k_{nr}=k-k_r$, where k is the observed rate constant for emission decay. It was assumed that the Arrhenius terms in Eq. (2) are negligible at these temperatures, making $k_{nr}=k^0_{nr}+k'_{nr}$. The emission energy (0–0 energy) was taken as the energy at the intensity maximum in the spectrum, which is a crude approximation, especially for the more distorted spectra. However, the error inflicted by the approximation cannot fully account for the displacement of the data points for **1a** and **3** from the line.

ferent ligands are usually only slightly affected when the other ligands are exchanged [12,37]. However, the present redox data were not conclusive in this respect (see below).

Two independent pieces of evidence are available from the emission properties that may help to identify the ligand involved in the lowest excited state. First, the emission spectra at 100 K show a well-resolved vibrational structure for all complexes except **1a** and **3** (Fig. 4). Second, the plot of ln k_{nr} vs. the emission energy, derived at 100 K and 140 K, is shown in Fig. 6 (energy gap law). All complexes, except **1a** and **3**, lie on the same line for both temperatures, suggesting that the emitting state has a common Ru–bpy ^{3}MLCT origin in these complexes [38]. The values for **1a** and **3** are clearly off this line, suggesting that they have a different origin, i.e. that the excitation is localized on the substituted bpy. In contrast, **1b** falls in with Ru(bpy)$_3^{2+}$ and the other complexes where the ^{3}MLCT state involves an unsubstituted bipyridine ligand. The correctness of using data for rigid and fluid solvents in the same correlation is supported by the results of Lumpkin and Meyer [24], who showed that the variation in k_{nr} is governed by the energy gap law through the whole region of the glass transition in ethanol–methanol for an osmium(II) polypyridine complex.

It is known that stretching vibrations of medium frequency ($h\nu \approx 1300$ cm^{-1}) in the bpy skeleton play a major role in the vibrationally induced deactivation of the excited state [29,38]. The substituents are likely to alter these vibrations. Indeed, the emission spectra at 100 K indicate a vibrational progression of lower frequency for **1a** and **3**. The structural distortion suggested by 2D NMR may lead to longer average Ru–N bonds. This would be expected to alter the deactivation contribution from Ru–N low-frequency vibrations ($h\nu \approx 400$ cm^{-1}) as well as the overlap between metal- and ligand-based orbitals. The loss of structure in the emission spectra of **1a** and **3** indicates that the medium frequency vibrations of the bpy ligands lose their dominance in the deactivation of the excited state due to the effects of the substituent. All these factors are expected to give differences in the energy gap law behaviour, and may explain the difference between **1a** and **3** and the other complexes in Fig. 6.

The emission blue shift and increase in vibrational structure on vitrification of the solvent have been suggested to be due to the inability of the solvent to reorganize sufficiently to allow localization (solvent trapping) of the excitation onto one ligand [39]. In this suggestion, it is assumed that the excitation is initially delocalized. However, there is evidence that localization occurs within 30 ps even in low-temperature glass [35,40]. Also, the same low-temperature spectrum is observed for Ru(bpy)$_3^{2+}$ and Ru(bpy)(2,2′-biisoquinoline)$_2^{2+}$ [41], and for Os(bpy)$_3^{2+}$ and Os(bpy)(1,2-dimethylarsinobenzene)$_2^{2+}$ [42]. In the latter complex, only the bipyridine ligand provides low-lying MLCT states; thus the excitation must be localized on a single ligand even at low temperature. The effect of vitrification on the emission spectrum may instead be explained by a reduced relaxation of the solvent and possibly a variation in the large-amplitude internal modes (Ru–N modes), resulting in a blue shift, and by a more uniform interaction with the rigid matrix, resulting in a more well-resolved spectral structure [24,43]. Thus the difference in vibrational structure at 100 K between the complexes in the present study does not originate from different degrees of localization of excitation.

It has been suggested [44] that, if the emission maximum of a heteroleptic complex is shifted to lower energies on protonation of a ligand, the excited state is localized on that ligand. While this is the case for the protonated ligand, it is not necessarily true that the unprotonated ligand provides lower ^{3}MLCT states than the other ligands. In the case of **1a** and **1b**, it seems that the excitation is localized on the carboxylate-bearing bpy (L1H), but when this is deprotonated (L1), the MLCT states of substituted bpy increase in energy above those of bpy itself, causing the excitation to be localized on the latter. The same reversal of state order was claimed for Ru(bpy)$_2$(4,4′-dicarboxy-bpy) on deprotonation [45].

We therefore assume that, for **1a** and **3**, the excited state is localized on the 6-substituted bpy, while it is bpy localized for all the other complexes, including **1b**. The assignments above are compatible with the redox data (Table 2), i.e. the ligand providing ^{3}MLCT states of lowest energy is also the easiest to reduce. However, in some cases, the situation is not clear. In **4**, we would expect the methyl substituent to decrease the reduction potential, and the last reduction does show a minor negative shift relative to Ru(bpy)$_3^{2+}$. In **2a** (**2b** could not be determined), the potentials of the first and third ligand reductions are shifted relative to Ru(bpy)$_3^{2+}$, but the shifts are small. For **3**, the potential for oxidation of the metal is increased slightly, while the potential for reduction of the first ligand changes from approximately -1.30 V to -1.19 V. This is in complete accordance with the fact that this ligand contains an electron-withdrawing group and that this ligand will be the dominant acceptor in the MLCT excited complex. For **1a**, no redox data are available because of interference

from water after the addition of trifluoroacetic acid (see Section 2, but the carboxy substituent would be expected to increase the electron acceptor properties of the ligand (L1H), as in **3**. For **1b**, the situation is not completely clear. Since the complex has a net charge of +1 instead of +2, all potentials would be expected to decrease. A comparison of the first and second ligand-based reductions of $Ru(bpy)_3^{2+}$ shows that the potential is shifted by approximately −200 mV when the first electron is added to give a net charge of +1. For **1b**, all three reduction potentials were shifted by about −200 mV relative to those of **3** (Table 2). This suggests that the ligands which bear the substituent are equally good electron acceptors in **1b** and **3**, and that both are better than bpy. However, an alternative line of reasoning is that the extra charge of the carboxylate ion in **1b** is unevenly distributed on the substituted bpy (L1), so that the unsubstituted bpy moieties are not equivalent. The bpy which is easiest to reduce also shows the smallest shift relative to $Ru(bpy)_3^{2+}$ (−110 mV). For the second bpy, the shift is a little larger (−170 mV) and, for L1, the largest (−210 mV). Based on the emission properties and the fact that deprotonation raises the π^*(6-carboxylato-bpy) levels above that of bpy [45], we tend to favour the second explanation. This implies that the substituted bipyridine L1 of **1b** is a poorer electron acceptor than bpy, and that the electron in the excited state is localized on one of the unsubstituted bipyridine ligands.

In conclusion, the emitting state was assigned to an Ru–bpy unit in all complexes except **1a** and **3**, where it was assumed that the substituted ligand was involved.

4.4. Photophysical behaviour

The dominating effects of the substituents on the photophysical properties originate from the steric repulsion between the substituent and the adjacent ligand. From 2D NMR, it is implied that the octahedral geometry of the complex is distorted (the appearance of NOEs requires breaking and lowering of the D_3 symmetry), which is known to reduce the ligand field strength. Thus the energy of the ^{3}MC state is reduced, so that deactivation through this state becomes important also at lower temperatures [12,29]. This explains the very short lifetime and low luminescence quantum yield at room temperature. Similar effects have been observed previously for ruthenium(II) complexes with 6,6′-substituted bipyridines [13–16].

Since the lifetimes were measured only at a few temperatures, no attempt was made to fit the data in Fig. 2 to an equation of the type shown in Eq. (2). However, it seems that all complexes, except perhaps **1a** and **1b** (see below), behave qualitatively in the same way as $Ru(bpy)_3^{2+}$. It can be noted that (Table 1, Fig. 4) steric distortion of the ground state from a pure octahedral D_3 $Ru(bpy)_3^{2+}$ configuration results in the following: (1) a red-shifted emission; (2) a larger k_{nr} value that is more sensitive to melting of the solvent, reducing both the emission lifetime and quantum yield; (3) a distorted shape of the emission spectrum (see Section 3); (4) a smaller ΔE_2 in Eq. (2); (5) a smaller extinction coefficient for the lowest transition to ^{1}MLCT, and a lower rate of radiative decay (Table 1), probably due to reduced Ru–bpy (d–π^*) orbital overlap. The distortion makes the Ru–N bonds longer, which is expected to result in weaker binding of the ligand and a larger difference in the equilibrium structure between the ground and excited states, which explains observations (2) and (3). The effect will be larger when the excitation is localized on ligands with more distorted geometry, i.e. in **1a** and **3**, as is observed. Generally, the complexes can be divided into three groups, where **5** is the reference, and the geometry is distorted in the other complexes (in **2** and **4** to a lesser extent than in **1** and **3**). The degree of perturbation of the photophysical properties from those of **5** follows the same pattern: **2** and **4** are less perturbed than **1** and **3**.

For **1b**, the emission lifetime and quantum yield do not change with temperature in a parallel manner, as shown in Fig. 3. This result implies that the rate constant for radiative decay k_r is significantly temperature dependent, even above 140 K. First, it must be pointed out that we carefully considered the possibility that a small fraction of less temperature sensitive impurity, e.g. $Ru(bpy)_3^{2+}$, was the cause of this observation. However, there would have had to be more than 10 mol.% of $Ru(bpy)_3^{2+}$ impurity to account for the observations, and the impurity level was determined to be lower than 2 mol.% (see Section 2). It should also be noted that the lifetimes of **1a** and **1b**, above 170 K, are sufficiently different such that a mixture of protonated and unprotonated forms in the sample can be excluded, since this would lead to deviations from a single exponential emission decay. Thus, in principle, there are two explanations for the temperature dependence of k_r: (1) during the excited state lifetime, there is a conformational change in the complex which alters the emission properties of the ^{3}MLCT state, and the relative rates of conformational change and excited state deactivation depend on the temperature; (2) there are one or more additional states present, with higher k_r, that are populated at higher temperatures.

A conformational change in the ^{3}MLCT state would result in a red shift of the emission during the excited state lifetime. No red shift would be observed, however, if the conformational change proceeded via non-emissive metal-centred states (see Section 1). At 160 K, there is no difference between the spectra recorded at less than 100 ns and 1000–1300 ns after the excitation pulse. This is to be expected since τ and Φ are essentially parallel up to this temperature (Fig. 3). At 170 K, τ and Φ start to deviate, but already at this temperature the low emission intensity and short lifetime preclude the recording of time-resolved emission spectra with the equipment available.

The other explanation for the change in k_r involves one or more additional ^{3}MLCT states populated at higher temperatures. Due to the unsymmetrically located 6-substituent, the unsubstituted bpy ligands are not equivalent. Thus the possible additional state (or states) may involve another ligand,

i.e. either the 6-carboxylato-bpy ligand (L1) or the bpy ligand which gives the ^{3}MLCT states of higher energy. Meyer and coworkers [45,46] predicted and showed that four ^{3}MLCT states, localized on the same ligand, are present for Ru(II) and Os(II) complexes of bpy. However, their results show that the fourth state is too high in energy to explain our observations, and for the present complexes it would not contribute to the excited state decay due to the dominance of decay through MC states at higher temperatures. In conclusion, we cannot, at this stage, discriminate between the two alternative explanations for the unusual temperature dependence of k_r for **1b**, although the explanation involving a conformational change seems less likely.

4.5. Possible ligand displacement reaction in the oxidized complexes

The possible intramolecular ligand displacement reaction induced by PET to a (hypothetical) acceptor in **1–3** leads to the formation of oxidized ruthenium complexes in the charge-separated state, as described in Section 1 (Scheme 1). Provided that the electronic coupling between the donor and acceptor is weak, the oxidized complexes **1–3** (without acceptors) may serve as models for the donor part of this charge-separated state. An exchange of ligands in the oxidized states of the complexes, resulting in coordination of the carbonyl or carboxylate group, would decrease the Ru(II/III) reduction potential by a few hundred millivolts [9]. This would lead to a large peak separation in the cyclic voltammetry experiments. Contrary to this expectation, our results showed no sign of the desired reaction: the oxidation of all complexes examined was reversible on the timescale of the experiments (of the order of seconds). Since this is several orders of magnitude longer than any presently observed lifetime for charge-separated states in molecular donor–acceptor systems, we conclude that the photoinduced intraligand displacement reaction proposed in Section 1 cannot occur in systems with **1–3** as donor parts.

5. Conclusions

We have reached a reasonable understanding of the excited state processes in the complexes studied. The emitting state in the heteroleptic complexes **1–4** was assigned using spectroscopic and electrochemical data. A gradual change in the photophysical properties was induced by the different substituents, where the most sterically distorted complexes **1** and **3** also exhibited the shortest excited state lifetimes. The abnormal photophysical behaviour of **1b**, displayed in Fig. 3, may be caused by the non-equivalence of the ligands, resulting in a significant population of MLCT states with different properties as the temperature is increased. We were unable to show any exchange of ligands in the oxidized complexes, as proposed in Section 1.

Acknowledgements

This is publication no. 2 from the Consortium for Studies of Artificial Photosynthesis, supported financially by the Knut and Alice Wallenberg Foundation. This work was also supported by NFR (Swedish Natural Science Research Council) and NUTEK (Swedish National Board for Industrial and Technical Development). T.N. acknowledges a personal grant from Vattenfall AB, Sweden. We thank Dr Stenbjörn Styring, Stockholm University, for stimulating discussions.

References

[1] T.J. Meyer, *Acc. Chem. Res.*, *22* (1989) 163. I. Willner and B. Willner, *Photoinduced Electron Transfer III*, Topics in Current Chemistry, Vol. 159, Springer-Verlag, Berlin, 1991, p. 153. J.S. Connoly, *Photochemical Conversion and Storage of Solar Energy*, Academic Press, New York, 1981. M. Grätzel (ed.), *Energy Resources through Photochemistry and Catalysis*, Academic Press, New York, 1983. T.J. Matsuo, *Photochemistry*, *29* (1985) 41.

[2] J. Deisenhofer and J.R. Norris, *The Photosynthetic Reaction Centre*, Vol. 2, Academic Press, San Diego, 1993.

[3] V. Balzani and F. Scandola, *Supramolecular Photochemistry*, Ellis Horwood, Chichester, 1991.

[4] D. Gust and T.A. Moore, *Photoinduced Electron Transfer III*, Topics in Current Chemistry, Vol. 159, Springer-Verlag, Berlin, 1991, p. 103.

[5] J.R. Bolton, N. Mataga and G. McLendon (eds.), *Electron Transfer in Inorganic, Organic and Biological Systems*, Advances in Chemistry Series, Vol. 228, American Chemical Society, Washington DC, 1991.

[6] V. Balzani and F. Scandola, *Supramolecular Photochemistry*, Ellis Horwood, Chichester, 1991, Chapter 7. W. Rettig, *Electron Transfer I*, Topics in Current Chemistry, Vol. 169, Springer-Verlag, Berlin, 1994, p. 253.

[7] T. Scherer, I.H.M. van Stokkum, A.M. Brouwer and J.M. Verhoeven, *J. Phys. Chem.*, *98* (1994) 10 539. N. Mataga, *Pure Appl. Chem.*, *65* (1993) 1605.

[8] Y. Kanda, H. Sato, T. Okada and N. Mataga, *Chem. Phys. Lett.*, *129* (1986) 306.

[9] A. Börje, T. Norrby, B. Åkermark, L. Hammarström, J. Alsins, K. Lashgari and R. Norrestam, manuscript in preparation.

[10] E.H. Yonemoto, R.L. Riley, Y.I. Kim, S.J. Atherton, R.H. Schmehl and T.E. Mallouk, *J. Am. Chem. Soc.*, *114* (1992) 8081. S.L. Larson, C.M. Elliott and D.F. Kelley, *J. Phys. Chem.*, *99* (1995) 6530.

[11] R.A. Marcus and N. Sutin, *Biochim. Biophys. Acta*, *811* (1985) 265.

[12] A. Juris, V. Balzani, F. Barigelletti, S. Campagna, P. Belser and A. von Zelewsky, *Coord. Chem. Rev.*, *84* (1988) 85.

[13] J.M. Kelly, C. Long, C.M. O'Connell, J.G. Vos and A.H.A. Tinnemans, *Inorg. Chem.*, *22* (1983) 2818.

[14] F. Barigelletti, A. Juris, V. Balzani, P. Belser and A. von Zelewsky, *Inorg. Chem.*, *22* (1983) 3335.

[15] D.A. Bardwell, F. Barigelletti, R.L. Cleary, L. Flamigni, M. Guardigli, J.C. Jeffrey and M.D. Ward, *Inorg. Chem.*, *34* (1995) 2438.

[16] R.H. Fabian, D.M. Klassen and R.W Sonntag, *Inorg. Chem.*, *19* (1980) 1977.

[17] A. Börje, T. Norrby, L. Zhang and B. Åkermark, manuscript in preparation.

[18] T.J. Meyer, D.J. Salmon and B.P. Sullivan, *Inorg. Chem.*, *17* (1987) 3334.

[19] T. Kauffmann, *Chem. Ber.*, *109* (1976) 3864. K.J. Schmalzl and L.A. Summers, *Aust. J. Chem.*, *30* (1977) 657.

[20] A. Börje, K. Lashgari, T. Norrby, R. Norrestam and B. Åkermark, manuscript in preparation.

[21] M.J. Cook, A.P. Lewis, G.S.G. McAuliffe, V. Skarda, A.J. Thomson, J.L. Glasper and D.J. Robbins, *J. Chem. Soc., Perkin Trans. II*, (1984) 1293.
[22] A. Börje, U. Jacobsson, T. Norrby and B. Åkermark, manuscript in preparation.
[23] B. Norden and S. Seth, *Appl. Spectrosc., 39* (1985) 647.
[24] R.S. Lumpkin and T.J. Meyer, *J. Phys. Chem., 90* (1986) 5307.
[25] J.N. Demas and G.A. Crosby, *J. Phys. Chem., 75* (1971) 991.
[26] N.E. Tokel-Takvoryan, R.E. Hemingway and A.J. Bard, *J. Am. Chem. Soc., 95* (1973) 6582.
[27] F.E. Lytle and D.M. Hercules, *Photochem. Photobiol., 13* (1971) 123.
[28] J.N. Demas and G.A. Crosby, *J. Am. Chem. Soc., 93* (1971) 2841.
[29] T.J. Meyer, *Pure Appl. Chem., 58* (1986) 1193.
[30] M.K. DeArmond and M.L. Myrick, *Acc. Chem. Res., 22* (1989) 364.
[31] J. van Houten and R.J. Watts, *Inorg. Chem., 17* (1978) 3381. D.P. Rillema, C.B. Blanton, R.J. Shaver, D.C. Jackman, M. Boldaji, S. Bundy, L.A. Worl and T.J. Meyer, *Inorg. Chem., 31* (1992) 1600. S. Tachiyashiki and K. Mizumachi, *Coord. Chem. Rev., 132* (1994) 113. S. Tachiyashiki, H. Ikezawa and K. Mizumachi, *Inorg. Chem., 33* (1994) 623.
[32] F. Barigelletti, A. Juris, V. Balzani, P. Belser and A. von Zelewsky, *J. Phys. Chem., 90* (1986) 5190.
[33] K. Kalyanasundaram, *Photochemistry of Polypyridine and Porphyrin Complexes*, Academic Press, London, 1992.
[34] R.A. Malone and D.F. Kelley, *Chem. Phys., 95* (1991) 8970.
[35] T. Yabe, D.R. Anderson, L.K. Orman, Y.J. Chang and J.B. Hopkins, *J. Phys. Chem., 93* (1989) 2302.
[36] D. Braun, P. Huber, J. Wudy, J. Schmidt and H. Yersin, *J. Phys. Chem., 98* (1994) 8044.
[37] C.M. Elliott and E.J. Hersenhart, *J. Am. Chem. Soc., 194* (1982) 7519. Y. Ohsawa, K.W. Hanck and M.K. DeArmond, *J. Electroanal. Chem., 175* (1984) 229.
[38] G.H. Allen, R.P. White, D.P. Rillema and T.J. Meyer, *J. Am. Chem. Soc., 106* (1984) 2613.
[39] J. Ferguson, E.R. Krausz and M. Maeder, *J. Phys. Chem., 89* (1985) 1852. N. Kitamura, H.-B. Kim, Y. Kawanishi, R. Obata and S. Tazuke, *J. Phys. Chem., 90* (1986) 1488.
[40] P.J. Carrol and L.E. Brus, *J. Am. Chem. Soc., 109* (1987) 7613.
[41] A. Juris, F. Barigelletti, V. Balzani, P. Belser and A. von Zelewsky, *Inorg. Chem., 24* (1985) 202.
[42] E. Danielson, R.S. Lumpkin and T.J. Meyer, *J. Phys. Chem., 91* (1987) 1305.
[43] F. Barigelletti, P. Belser, A. von Zelewsky, A. Juris and V. Balzani, *J. Phys. Chem., 89* (1985) 3680.
[44] J.G. Vos, *Polyhedron, 11* (1992) 2285.
[45] R.S. Lumpkin, E.M. Kober, L.A. Worl, Z. Murtaza and T.J. Meyer, *J. Phys. Chem., 94* (1990) 239.
[46] E.M. Kober and T.J. Meyer, *Inorg. Chem., 23* (1984) 3877.